Hindawi
Mathematical Problems in Engineering
Volume 2022, Article ID 9692047, 13 pages
https://doi.org/10.1155/2022/9692047

Research Article

Regional Financial Economic Data Processing Based on Distributed Decoding Technology

HuiLi Zhang

Yellow River Conservancy Technical Institute, Kaifeng 475000, China

Correspondence should be addressed to HuiLi Zhang; zhanghuili@yrcti.edu.cn

Received 18 April 2022; Accepted 17 May 2022; Published 8 June 2022

Academic Editor: Wei Liu

To improve the effect of regional financial and economic data processing, this study combines the distributed decoding technology to construct the regional financial data processing system. Furthermore, this study combines the technical characteristics of cooperative communication and unitary space-time codes to design a non-differential distributed space-time code based on cyclic unitary matrix groups. In addition, this study uses the particularity of trigonometric functions to design a non-differential distributed space-time code based on trigonometric functions. Finally, according to the characteristics of the distributed space-time code of trigonometric functions, this study obtains a decoding algorithm with low decoding complexity and uses MATLAB to conduct simulation experiments to verify the financial data processing and economic analysis effect of the system in this study. The experimental analysis results show that the regional financial and economic data processing system based on distributed decoding technology proposed in this study can play an important role in the analysis of financial and economic data.

1. Introduction

The Internet financial data mining system obtains the required financial data from a specific financial website and then performs a series of extraction processing on these financial data to form structured financial data, which are stored in the database of the target server for query and use by users dealing with financial services. In the current complex economic situation at home and abroad, people need to use the open network to obtain real-time and effective financial data. The Internet financial data collection and analysis system can provide enterprises or individual users with real-time and accurate financial data through the Internet, so that users can observe the data changes in various financial information in real time and obtain the most humanized information recommendation, and it provides a data basis for users to carry out various financial business activities. At the same time, under the current complex economic situation at home and abroad, people need to obtain a large amount of data to realize accurate mining of financial data. Therefore, it is very necessary to design an efficient, simple, and accurate Internet financial data mining system.

How to obtain the required information on a specific website, store the useful information, and display it in a certain form is beneficial to the financial data research, which makes the Web financial data mining technology a hot spot of current research. Since the establishment of China's security market for more than ten years, with the continuous development of computer technology, informatization, and networking, various financial institutions in the financial industry have stored and accumulated a large amount of original financial data. How to continuously improve financial data mining management has also become a problem. It has become a hot topic. At present, multidimensional data are ubiquitous, especially in the economic field. The cumbersome multidimensional financial data bring great difficulties to users' analysis and understanding. With the increasing capacity and complexity of financial data, traditional visualization technology is difficult to meet the needs of users. Fast and convenient visualization and analysis of multidimensional information data have become a research hotspot in the financial field.

To effectively improve the cognitive law of parallel coordinates and reduce visual clutter, clustering is widely used

in various fields, and most of the clustering methods are based on single data or based on visual space. Data-based clustering is to preprocess and classify the data before drawing, but due to the large range of the dataset, the results drawn in parallel coordinates after clustering may still be very messy, and it is difficult to identify the data characteristics of each classification and trends. The clustering method based on visual space transforms and classifies by analyzing the geometric relationship between line segments in parallel coordinates, which often leads to the clustering results without considering the actual meaning of the data itself, which affects the accuracy of clustering. Since the single visual space-based clustering method simply relies on the results of the visualization of parallel coordinates, clustering by analyzing the geometric relationship between line segments does not integrate the meaning represented by the data itself, which reduces the accuracy of classification to a certain extent and affects the application and promotion of parallel coordinate technology in the financial field.

This study combines distributed decoding technology to construct a regional financial data processing system to improve the effect of regional financial data processing and promote the reliability of financial analysis.

2. Related Work

Traditional financial data analysis methods mainly use mathematical statistics to establish corresponding mathematical-statistical models for analysis and prediction [1]. The proposed multivariate discriminant analysis model for financial data is also known as the Z score model [2]. The multiple discriminant analysis model is to select one or two most representative indicators from the indicators such as asset liquidity, profitability, solvency, and operating capacity. The coefficients in the model are relative to each indicator obtained according to the statistical results. Measure of importance: a large number of empirical studies have shown that the model has a good early warning function for corporate financial crisis [3]. However, its prediction effect is also different due to the length of time. The shorter the prediction period, the stronger the prediction ability. Therefore, this model is more suitable for the judgment of short-term risks of enterprises. According to Altman's financial ratio discriminant analysis model to expand and improve, the financial ratio discriminant analysis and logit regression method are used to establish and estimate the early warning model, and a good prediction effect has been achieved [4]; the component financial early warning model, because the principal component analysis method in the field of artificial intelligence is introduced into the judgment model, improves the rationality of the selection of indicators, thus greatly improving the accuracy of financial early warning [5]. For financial time-series data, commonly used statistical analysis methods include autoregressive moving average model, correlation coefficient analysis, asset pricing portfolio analysis, and ARCH model analysis. Among them, the ARCH model is considered to be the most concentrated model that reflects the characteristics of variance changes and is widely used in the time-series analysis of financial data. It is the most important innovation in the development of financial econometrics [6]. Among all volatility models, ARCH models are unique in terms of the depth of theoretical research and the breadth of empirical application. These analysis methods play an objective and quantitative analysis role in the study of financial markets and corporate financial status, so they have been widely used [7]. Usually, the method of data statistics is used to establish a mathematical model. It must be assumed in advance that the observed data satisfy a certain type of model, and then, statistical tests are used to determine whether the assumed model conforms to the actual situation of the data. If it does not conform, the model must be adjusted until predictive analysis can only be performed if the assumptions are met [8]. Every mathematical model is established under certain constraints and only applies to a specific range. The financial market is a complex dynamic system, so a statistical model determined only by limited parameters cannot be comprehensive and accurate. To describe the real situation of the market, it cannot effectively predict the future development trend of the market [9]. In recent years, machine learning methods, data mining methods, and related dynamic methods in the field of artificial intelligence have been unprecedentedly developed, and data analysis methods based on artificial intelligence have also been effectively and widely used in the financial field [10].

On the basis of the original industrial theoretical model, the relationship between financial agglomeration and the industrial structure formed by financial development is studied [11]; the combination of financial big data and algorithms provides an ideal technical foundation for the transformation and upgrading of traditional financial services. The perspective of different types of financial structures to study their impact on the industry [12]. The combination of the two provides an ideal technological foundation for the transformation and upgrading of traditional financial services. In the field of banking and finance, big data financial algorithms are widely used in customer marketing, product innovation, risk control, operation optimization, etc. [13]; through the algorithmic processing of customer financial information, a panoramic portrait of customers is obtained and the acquisition rate of new customers is improved. The marketing model of financial business is improved through cross-marketing algorithm analysis, precision marketing algorithm analysis, personalized recommendation algorithm analysis, etc.; through financial market risk algorithm analysis, SME risk assessment algorithm analysis, real-time fraud transaction algorithm analysis, anti-money laundering activity algorithm analysis, etc., to improve financial risk management and control capabilities [14]; and through channel optimization algorithm analysis, market hotspot algorithm analysis, and other big data methods to optimize the quality of financial operations. In the field of securities, the widespread application of artificial intelligence investment advisors driven by big data financial algorithms has become an important business model for modern security trading [15]. In the insurance industry, big data financial algorithms play an important role in insurance innovation, customer marketing, effective use of insurance funds, and risk control. In traditional financial fields such as the trust industry, financial leasing industry, and guarantee industry, big data financial algorithms are also constantly optimizing and reconstructing the business

model of traditional finance. The field has gained a broad application space [16].

3. Distributed Decoding Technology

A non-differential distributed unitary space-time coding based on a cyclic unitary matrix group is proposed, and a partially coherent distributed differential code under the multi-hop model is constructed. The performance comparison of two-hop and multi-hop modes is analyzed and compared, and it is concluded that the system performance in multi-hop mode is better at a high signal-to-noise ratio.

Definition 1. we assume that a is an element of group G, and the smallest positive integer n that makes $a^n = e$ (identity element of group G) is called the order of element a. The order of an element a is usually represented by $|a|$.

Definition 2. we assume that G is a group and H is a non-empty subset of G. If the multiplication of G by H itself also acts as a group, it is called a subgroup of G.

Definition 3. if a group G can be generated by an element a, that is, $G = \langle a \rangle$, then G is called a cyclic group generated by a, and this process is called a generator of G [17].

Definition 4. we assume that $\langle a^n \rangle$ is a cyclic group of finite order then the power of the element with base a is called the element index of the cyclic group.

Lemma 1. *we assume that the order of the element a in the group G is n, and then,* $a^m = e \Leftrightarrow n|m$.

Lemma 2. *if the order of element a in the group is n, then* $|a^k| = n/(k, n)$ *1, where k is any integer.*

Lemma 3. *a subgroup of a cyclic group is also a cyclic group.*

We assume that Ω *is the set of L different west matrices; that is,* $\Omega = \{\mathbf{u}_1, \mathbf{u}_2, \ldots, \mathbf{u}_{L-1}\}$.

The easiest way to construct a commutative group with L elements is to construct a cyclic group; that is,

$$\mathbf{u}_l = \mathbf{u}_1^l, \tag{1}$$

where $\mathbf{u}_1$ is the generator matrix of the cyclic group, and it is a diagonal matrix, which can be expressed as follows:

$$\mathbf{u}_1 = \begin{bmatrix} e^{j\frac{2\pi}{L}u_1} & 0 & \cdots & 0 \\ 0 & e^{j\frac{2\pi}{L}u_2} & \cdots & 0 \\ \vdots & \vdots & \ddots & \vdots \\ 0 & 0 & \cdots & e^{j\frac{2\pi}{L}u_k} \end{bmatrix}. \tag{2}$$

In the formula, $u_k \in \{0, 1, \ldots, L-1\}, k = 1, 2, \ldots, m$.

Then, any element in the cyclic group can be expressed as follows:

$$\mathbf{u}_l = \begin{bmatrix} e^{j\frac{2\pi}{L}u_l l} & 0 & \cdots & 0 \\ 0 & e^{j\frac{2\pi}{L}u_2 l} & \cdots & 0 \\ \vdots & \vdots & \ddots & \vdots \\ 0 & 0 & \cdots & e^{j\frac{2\pi}{L}u_k l} \end{bmatrix}, l = 1, 2, \ldots, L-1. \tag{3}$$

The source node maps $\log_2 L$ bits of information to a certain matrix of the Ω set. Without loss of generality, we apply the following formula when constructing a circulant matrix [18]:

$$\mathbf{\Phi}_l = \mathbf{\Theta}' \mathbf{\Phi}_0. \tag{4}$$

In this study, $\Theta = \mathbf{u}_1$, and then, $\Theta' = \mathbf{u}_l = \mathbf{u}_1^l$. Because the system models built in this section have only one source node, we assume that Φ_0 is a column vector, which can be expressed as $\Phi_0 = 1/\sqrt{m}\begin{bmatrix} 1 & 1 & \cdots & 1 \end{bmatrix}^T$.

Then, the transmission matrix can be expressed as follows:

$$\mathbf{\Phi}_l = \frac{1}{\sqrt{m}} \begin{bmatrix} e^{j\frac{2\pi}{L}u_l l} & e^{j\frac{2\pi}{L}u_2 l} & \ldots & e^{j\frac{2\pi}{L}u_l l} \end{bmatrix}^{\mathrm{T}}. \tag{5}$$

To get better system performance, we need to obtain the optimal parameters $u_1, u_2, \ldots, u_k$ and obtain the optimal constellation, and the constellation parameter group is denoted as the vector $\mathbf{v}$.

Without loss of generality, $0 \le u_1, u_2, \ldots, u_k \le L-1$ is set, which is chosen in this study according to the following criteria:

$$\begin{aligned} &\min_{0 \le u_1, \ldots, u_k \le L-1 l=2,\ldots,L} \max_k \frac{1}{k} \sum_{i=1}^{k} \exp\left[j \frac{2\pi}{L} u_i l \right] \\ &\quad = \min_{0 \le u_1, \ldots, u_k \le L-1} \delta. \end{aligned} \tag{6}$$

In the formula, $\delta \triangleq {}_{1 \le 1 \le L} \| {\Phi_0}^H \Phi_{\mathbf{k}} \|$. To associate δ with the singular value $\| {\Phi_0}^H \Phi_k \|$, we assume that μ is the mean of the squares of these singular values; that is, $\mu = (1/N_t) \sum_{i=1}^{N_t} \nu_i^2 = \| {\Phi_0}^H \Phi_k \|^2$, so that $\delta = \sqrt{\mu}$. For a given fixed mean μ, the error probability is minimized when the singular values are equal (i.e., uniformly distributed). Therefore, if two groups have the same δ, the group of parameters with more agreement should be selected.

As shown in Figure 1, in the first stage of cooperative communication, the source node P_1 transmits the code words in the codebook $S = \{\mathbf{s}_1, \mathbf{s}_2, \mathbf{s}_3, \ldots, \mathbf{s}_L\}$ with transmit power, where $E[{\mathbf{s}_l}^H \mathbf{s}_l] = 1$. The signal received by the ith relay node can be expressed as follows:

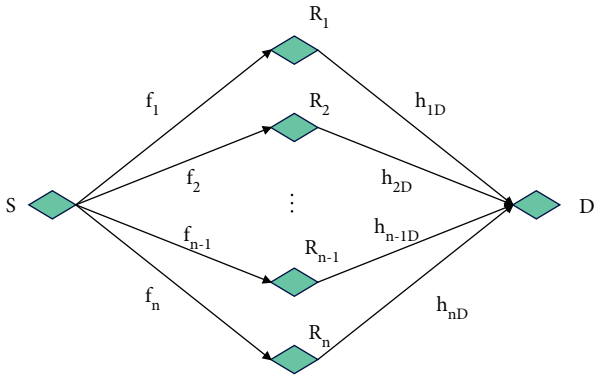

Figure 1: Multi-relay two-hop cooperative system model.

$$\mathbf{y}_{s,r_i} = \sqrt{P_1} f_i \mathbf{s} + \mathbf{v}_i, i = 1, 2, \ldots, n. \tag{7}$$

In the second stage, the information obtained after the relay node performs linear processing on the received information can be expressed as $t_i = \sqrt{P_2/N_0 + \delta^2_{s,r_i} P_1}\mathbf{y}_{s,r_i}\mathbf{A}_i$, and then, all n relay nodes simultaneously forward the processed information t_i to the destination node D with power P_2. Among them, $\mathbf{A}_i$ is the west matrix constructed according to the Hadamard matrix criterion.

The signal received by destination node D can be expressed as [19]follows:

$$\mathbf{y}_D = \sum_{i=1}^{n} h_{iD}\mathbf{t}_i + \mathbf{w} = \sqrt{\frac{P_1 P_2}{N_0 + \delta^2_{s,r_i} P_1}}\mathbf{S}\mathbf{h} + \mathbf{w}, i = 1, 2, \ldots, n. \tag{8}$$

In the formula, $\mathbf{w}$ is additive white Gaussian noise, which obeys a cyclic symmetric Gaussian distribution with mean 0 and variance δ^2. The equivalent channel coefficient $\mathbf{h}$ can be expressed as $\mathbf{h} = [\, f_1 h_1 \;\; f_2 h_2 \;\; \cdots \;\; f_n h_n \,]^T$. The code word sent by the relay end is expressed as $\mathbf{S} = [\, \mathbf{A}_1\mathbf{s} \;\; \mathbf{A}_2\mathbf{S} \;\; \cdots \;\; \mathbf{A}_n\mathbf{s} \,]$.

The signal matrix decoded by the maximum-likelihood decoding algorithm can be expressed as follows:

$$P(\mathbf{Y}|\mathbf{S}) = \frac{\exp\left(-tr\left\{\left(\mathbf{I}_T + \mathbf{S}\mathbf{S}\mathbf{S}^H\right)^{-1}\mathbf{Y}\mathbf{Y}^H\right\}\right)}{\pi\left|\mathbf{I}_T + \mathbf{S}\mathbf{S}^H\right|}. \tag{9}$$

The signal matrix decoded by the maximum-likelihood decoding algorithm can be expressed as follows:

$$\widehat{\mathbf{S}} = \arg\max P(\mathbf{y}|\mathbf{S}, h_i). \tag{10}$$

According to formula (5) and formula (6), formula (10) is simplified, and the maximum-likelihood decoding in the partially coherent two-hop network is obtained, as follows:

$$\widehat{\mathbf{S}} = \arg\max\left(\mathbf{y}^H\mathbf{S}\Lambda\mathbf{K}\mathbf{S}^H\mathbf{y}\right). \tag{11}$$

In the formula, $\Lambda = \mathrm{diag}(\eta_1, \eta_2, \ldots, \eta_n)$, $\eta_i = |h_i|^2\,(|h_i|^2 + \alpha\beta^{-1})^{-1}$, $\alpha = (1 + (P_2/1 + P_1)\sum_{i=1}^{n}|h_i|^2)\;\mathbf{I}_T$, $\beta = (P_1P_2T/1 + P_1)$.

According to formula (11), it can be equivalent to as follows:

$$\arg\max_{k\in 1,2,..L}\left(\mathbf{y}_1^H\Lambda_1\mathbf{y}_1 + Re\left\{\mathbf{y}_1^H\Lambda_2\mathbf{y}_2\right\} + \mathbf{y}_2^H\Lambda_3\mathbf{y}_2\right). \tag{12}$$

Among them, $\mathbf{y}_1 = [\, y_1 \;\; y_2 \;\; \cdots \;\; y_R \,]^T$, $\mathbf{y}_2 = [\, y_{R+1} \;\; y_{R+2} \;\; \cdots \;\; y_{2R} \,]^T$, $\Lambda_1 = \gamma_1 \odot \Omega$, $\Lambda_2 = \gamma_2 \odot \Omega$, $\Lambda_3 = \gamma_3 \odot \Omega$, $[\gamma_1]_{i,j} = \omega^{(u_l - u_j)k}$, $[\gamma_2]_{i,j} = \omega^{(u_l - u_{R+j})^k}$, and $[\gamma_3]_{i,j} = \omega^{(u_{R+t} - u_{R+j})^k}$, Ω is a Hermitian matrix of $n \times n$, and the ith row j column in the matrix is $\Omega_{i,j} = \sum_{\lambda=1}^{n}(\eta_\lambda m_{i\lambda} m^*_{j\lambda})$, $i, j = 1, \ldots, n$, $\eta_i = |h_i|^2\,(|h_i|^2 + \alpha\beta^{-1})^{-1}$, $j = 1, \ldots, R$.

To verify that the selection of the parameter matrix has a certain influence on the performance of the west space-time coding, $L = 16$ is selected. The channel coefficient and noise are both independent and identically distributed complex Gaussian random variables with mean 0 and variance 1. Both the source node and the destination node are one antenna, and there are four antennas at the relay to participate in the cooperation. Five groups of different parameter matrices were selected, $\mathbf{v} = [\, 5 \;\; 5 \;\; 5 \;\; 5 \,]$, $\mathbf{v} = [\, 1 \;\; 3 \;\; 5 \;\; 7 \,]$, $\mathbf{v} = [\, 1 \;\; 11 \;\; 13 \;\; 15 \,]$, $\mathbf{v} = [\, 5 \;\; 5 \;\; 11 \;\; 13 \,]$, $\mathbf{v} = [\, 7 \;\; 11 \;\; 13 \;\; 15 \,]$. The performance simulation results are shown in Figure 2.

Comparing the non-differential cyclic unitary matrix group code with the differential cyclic group code, the simulation result of the bit error rate is shown in Figure 3. The results show that the differential coding does not require channel estimation in the decoding process, which saves the time and power of sending training sequences, but its performance is about 3 dB worse than that of coherent distributed space-time coding.

In the actual communication environment, sometimes the two communication devices do not have the conditions for direct communication, and the communication between the source node and the destination node must rely on multiple relay nodes to be forwarded many times before it can be realized. This is the multi-hop relay in cooperative communication. The multi-hop relay cooperative communication model is shown in Figure 4.

A multi-hop non-differential distributed space-time code based on unitary group code is proposed, and the three-hop communication system model is shown in Figure 5.

In this model, we assume that the wireless communication system has $m + n + 2$ nodes, one of which is the source node and the other is the destination node, and $m + n$ relay nodes assist the source node to communicate. Among them, m is the number of first-hop relay nodes and n is the number of second-hop relay nodes. The whole communication process can be divided into three stages. In the first stage, the source node transmits the signal to the relay node R_{1i}. The signal received at the ith relay node is represented as follows:

$$\mathbf{y}_{s,r_{1i}} = \sqrt{P_1} f_i \mathbf{s} + \mathbf{v}_i, i = 1, 2, \ldots, m. \tag{13}$$

In the formula, $\mathbf{s}$ is an $L \times 1$-dimensional transmission data vector under the power constraint condition $\|\mathbf{s}\|_F^2 \le L$, where $L = n$, and $\|\cdot\|_F^2$ represents the Frobenius norm. Without loss of generality, we assume that the channel of the relay node is symmetric; that is, for $\forall i$, $f_i \sim \mathrm{CN}(0, \delta^2_{s,r_i})$ represents the channel gain between the source node and the R_{1i}th relay node.

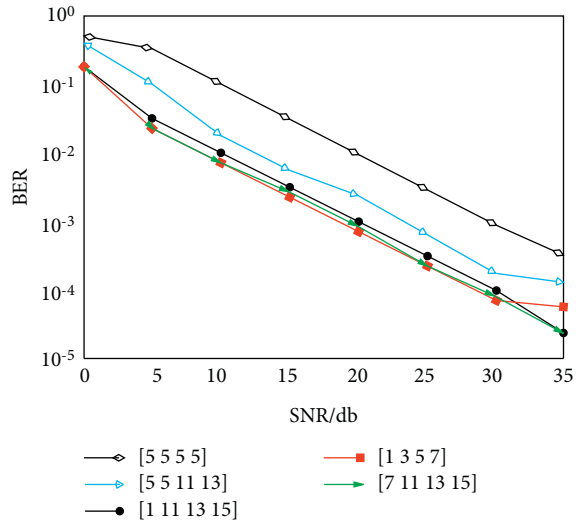

Figure 2: In the two-hop cooperative communication, $L = 16$, the performance comparison of different parameter matrices.

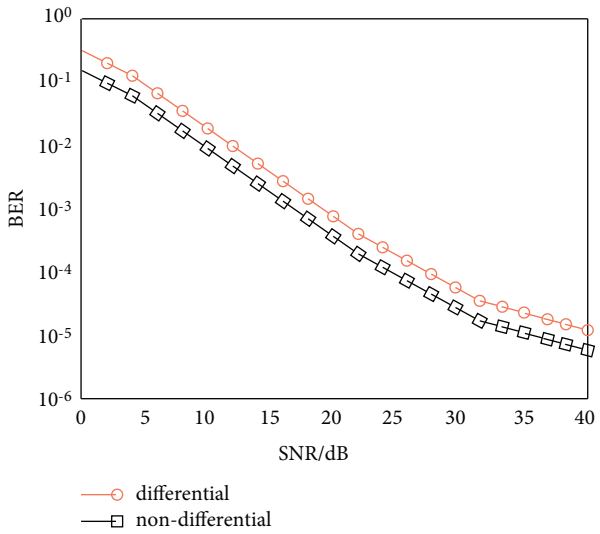

Figure 3: In the two-hop cooperative communication, $L = 16$, the performance comparison of differential and non-differential coding.

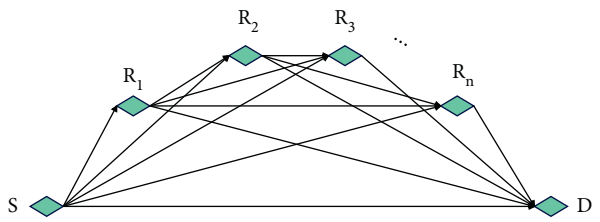

Figure 4: Cooperative communication model under multi-hop and multi-relay.

In the second stage, the relay node R_{1i} sends the received signal to the relay node R_{2j} after linear processing. This uses $\mathbf{A}_i$ to represent the west transformation matrix at the ith

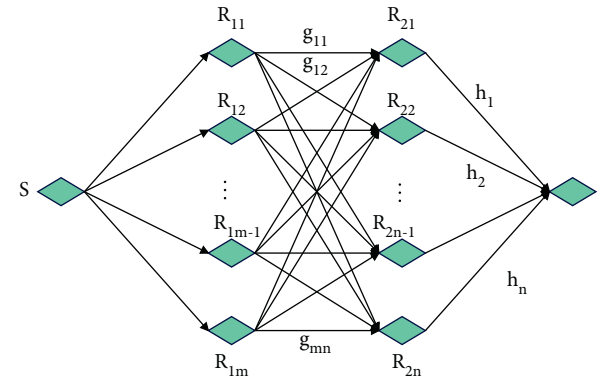

Figure 5: System model of a three-hop communication network.

relay node. In addition, the power of the received signal needs to be normalized to ensure that the signal sent from the relay node can meet the power limit condition. Normalizing this ensures that the average transmit power per symbol is $P = P_1 + P_2$. The signal after linear processing is $\mathbf{t}_i = \sqrt{P_2/N_0 + \delta^2_{s,r_i} P_1}\mathbf{y}_{s,r_i}\mathbf{A}_i$, where P_2 is the average transmit power of each relay, and the processed signal is sent to R_{2j}.

The signal received at relay node R_{2j} is as follows:

$$y_{r_{2j}} = \sum_{i=1}^{m} g_{ij}\mathbf{t}_i + \mathbf{w}_j = \sqrt{\frac{P_1 P_2}{N_0 + \delta^2_{s,r_i} P_1}}\mathbf{S}_1\mathbf{h}_j + \mathbf{w}, j = 1, 2, \ldots, n. \tag{14}$$

In the formula, the equivalent channel is $\mathbf{h}_j = \left[f_1 g_{1j} \;\; f_2 g_{2j} \;\; \cdots \;\; f_m g_{mj} \right]^T$, $\mathbf{w} = \sqrt{P_2/N_0 + \delta^2_{s,r_i} P_1}\left(\sum_{i=1}^{m} g_{ij}\mathbf{v}_i\mathbf{A}_i\right) + \mathbf{w}_j$, $\mathbf{w}_j$ is the noise vector at the relay node R_{2j}, and $\mathbf{w}$ is the additive white Gaussian noise at the node, which includes the noise forwarded from the relay node R_{1i} and the noise at the node itself. Therefore, the linear transformation at the relay node is finally selected

as the west linear transformation to ensure that the noises w are independent of each other. The code word matrix $S_1 = [\mathbf{A}_1 s \ \ A_2 s \ \cdots \ A_m s]$ in the formula reflects the role of distributed space-time code here.

In the third stage, the relay node R_{2j} sends the received signal through the west linear transformation again, and $\mathbf{B}_j$ represents the west transformation matrix at the jth relay node. The signal after the western linear transformation is as follows:

$$\tilde{\mathbf{y}}_{r_{2j}} = \sqrt{\frac{P_3}{N_0 + \delta^2_{s,r_{it}} P_1 + m\delta^2_{r_i,r_{2j}} P_2}}\, \mathbf{y}_{r_{r_j}} \mathbf{B}_j. \tag{15}$$

In the formula, P_3 is the average transmit power of each relay in the relay node, and the processed signal is sent to the destination node D.

Then, the signal received by destination node D is as follows:

$$\begin{aligned}\mathbf{y}_D &= \sum_{j=1}^{n} \tilde{\mathbf{y}}_{r_{2j}} h_j + \mathbf{v}_d \\ &= \sqrt{abP_1}\,[\, f_1\mathbf{A}_1 s \ \ f_2\mathbf{A}_2 s \ \cdots \ f_m\mathbf{A}_m s\,] \begin{bmatrix} g_{11} & g_{12} & \cdots & g_{1n} \\ g_{21} & g_{22} & \cdots & g_{2n} \\ \cdots & \cdots & \cdots & \cdots \\ g_{m1} & g_{m2} & \cdots & g_{mn} \end{bmatrix} \\ &\quad \cdot [\, \mathbf{B}_1 h_1 \ \ \mathbf{B}_2 h_2 \ \cdots \ \mathbf{B}_n h_n \,]^{\mathrm{T}} + \mathbf{n},\ j = 1, 2, \ldots, n.\end{aligned} \tag{16}$$

According to the equivalent transformation of the matrix, the above formula can be transformed into

$$\begin{aligned}\mathbf{y}_{\mathrm{D}} &= \sqrt{abP_1}\,[\, \mathbf{A}_1 s \ \ \mathbf{A}_2 s \ \cdots \ \mathbf{A}_m s\,] \begin{bmatrix} f_1 \\ f_2 \\ \ddots \\ f_m \end{bmatrix} \begin{bmatrix} g_{11} & g_{12} & \cdots & g_{1n} \\ g_{21} & g_{22} & \cdots & g_{2n} \\ \cdots & \cdots & \cdots & \cdots \\ g_{m1} & g_{m2} & \cdots & g_{mn} \end{bmatrix} \begin{bmatrix} \mathbf{B}_1 & & & \\ & \mathbf{B}_2 & & \\ & & \ddots & \\ & & & \mathbf{B}_n \end{bmatrix} \begin{bmatrix} h_1 \\ h_2 \\ \vdots \\ h_n \end{bmatrix} + \mathbf{n} \\ &= \sqrt{abP_1}\,[\, \mathbf{A}_1 s \ \ \mathbf{A}_2 s \ \cdots \ \mathbf{A}_m s\,] [\, \Lambda_1 \ \ \Lambda_2 \ \cdots \ \Lambda_i\,] \begin{bmatrix} \Psi_1 \\ \Psi_2 \\ \ddots \\ \Psi_i \end{bmatrix} \begin{bmatrix} h_1 \\ h_2 \\ \vdots \\ h_n \end{bmatrix} + \mathbf{n} \\ &= \sqrt{abP_1}\mathbf{S}\mathbf{H} + \mathbf{n}, i = 1, 2, \ldots, n.\end{aligned} \tag{17}$$

In the formula, there are

$$a = \frac{P_2}{N_0 + \delta^2_{s,r_{1i}} P_1}, b = \frac{P_3}{N_0 + \delta^2_{s,r_{ii}} P_1 + m\delta^2_{r_{i,},r_{2j}} P_2}, \Lambda_i = diag\left[\underbrace{\mathbf{B}_i \mathbf{B} \ldots \mathbf{B}_i}_{m \text{ individual}}\right], \tag{18}$$

$$\Psi_i = [\, f_1 g_{1i} \ \ f_2 g_{2i} \ \cdots \ f_m g_{mi}\,]^T, \mathbf{n} = \sqrt{ab} \sum_{j=1}^{n} \sum_{i=1}^{m} g_{ij} \mathbf{v}_i \mathbf{A}_i \mathbf{B}_j h_j + \sqrt{b} \sum_{j=1}^{n} w_j \mathbf{B}_j h_j + \mathbf{v}_d,$$

$$\mathbf{S} = [\, \mathbf{s}_1 \ \ \mathbf{s}_2 \ \cdots \ \mathbf{s}_n\,], \mathbf{s}_i = [\, \mathbf{A}_1 \mathbf{B}_i s \ \ \mathbf{A}_2 \mathbf{B}_i s \ \cdots \ \mathbf{A}_m \mathbf{B}_i s\,], \tag{19}$$

$$\mathbf{H} = [\, \mathbf{h}_1 \ \ \mathbf{h}_2 \ \cdots \ \mathbf{h}_i\,]^T, \mathbf{h}_i = [\, f_1 g_{1i} h_i \ \ f_2 g_{2i} h_i \ \cdots \ f_m g_{mi} h_i\,]^T, i = 1, 2, \ldots, n. \tag{20}$$

For the generalized Butson–Hadamard matrices, $\mathbf{M}\mathbf{M}^H = \mathbf{M}^H\mathbf{M} = \gamma \mathbf{I}_T$ must be satisfied, where $\mathbf{M}$ is an $\gamma \times \gamma$-dimensional matrix whose elements satisfy $m_{ij}{}^* = m_{ij}{}^{-1}$.

In this section, we assume that D is a generalized Butson–Hadamard matrix of $m \times m$, and matrix D is used to construct a diagonal west matrix $\mathbf{A}_i$, such that $\mathbf{A}_i = \mathrm{diag}(\mathbf{D}_{1i}\mathbf{D}_{2i} \ldots \mathbf{D}_{mi}), i = 1, 2 \ldots m$. Each of the diagonal elements $\mathbf{D}_{ij}$ is the element of the ith row and the jth column of the matrix D.

The first-hop relay node sends the vector $\mathbf{A}_i \Phi_k$ of $m \times 1$ to the second-hop relay node, that is, $\mathbf{S}_1$ in formula (14), which is recorded as follows:

$$\mathbf{S}_{k1} = \left[\, \mathbf{A}_1\mathbf{\Phi}_k \;\; \mathbf{A}_2\mathbf{\Phi}_k \;\; \cdots \;\; \mathbf{A}_m\mathbf{\Phi}_k \,\right] = \frac{1}{\sqrt{m}}\mathbf{\Theta}^k\mathbf{D}, k = 1, 2, \ldots, L. \tag{21}$$

In the formula, $\mathbf{S}_{k1}$ satisfies $\mathbf{S}_{k1}{}^{\mathrm{H}}\mathbf{S}_{k1} = \mathbf{I}_m$.

In the same way, the second-hop relay matrix $\mathbf{B}_j$ is designed. We assume that $\mathbf{G}$ is a generalized Butson–Hadamard matrix of $m \times m$ dimension, and the matrix $\mathbf{G}$ is used to construct the diagonal west matrix $\mathbf{B}_j$, so that $\mathbf{B}_j = \mathrm{diag}\left(\, \mathbf{G}_{1j} \;\; \mathbf{G}_{2j} \;\; \cdots \;\; \mathbf{G}_{mj} \,\right), j = 1, 2 \ldots m$, where each diagonal element $\mathbf{G}_{ij}$ is the element in the ith row and the jth column of the matrix $\mathbf{G}$. Then, the second-hop relay node sends $\mathbf{B}_j\mathbf{S}_{k1}$ to the destination node; that is, $\mathbf{S}$ in formula (17) is obtained, as shown as follows:

$$\mathbf{S}_k = \left[\, \mathbf{B}_1\mathbf{S}_{k1} \;\; \mathbf{B}_2\mathbf{S}_{k1} \;\; \cdots \;\; \mathbf{B}_m\mathbf{S}_{k1} \,\right] = \left[\, \mathbf{\Psi}_{k1} \;\; \mathbf{\Psi}_{k2} \;\; \cdots \;\; \psi_{kn} \,\right]. \tag{22}$$

In the formula, $\Psi_{kj} = \left[\, \mathbf{A}_1\mathbf{B}_j\Phi_k \;\; \mathbf{A}_2\mathbf{B}_j\Phi_k \;\; \cdots \;\; \mathbf{A}_n \;\; \mathbf{B}_j\Phi_k \right], j = 1, 2, \ldots, n$.

The relay matrices A_i, B_j in formula (16) are west matrices, and the random vectors $\mathbf{v}_i, \mathbf{w}_j$, and $\mathbf{v}_d$ all obey the Gaussian distribution, and they are independent of each other. We assume that the number of relay nodes in the first hop is the same as the number of relay points in the second hop; that is, $m = n = R$.

Then, the covariance matrix of additive noise is as follows:

$$\begin{aligned} E[\mathbf{n}] &= \mathbf{0}_T, \\ E\left[\mathbf{n}\mathbf{n}^H\right] &= \left(ab\sum_{i=1}^{m}\sum_{j=1}^{n}\left|g_{ij}h_j\right|^2 + b\sum_{j=1}^{n}\left|h_j\right|^2 + 1 \right)\mathbf{I}_T = \xi\mathbf{I}_T. \end{aligned} \tag{23}$$

Since this study is based on a partially coherent network, we assume that the destination node only knows about g_{ij} and h_j but not f_i. From this, it can be concluded that

$$\begin{aligned} E[\mathbf{y}|\mathbf{S}, g_i, h_i] &= \mathbf{0}_T, \\ E\left[\mathbf{y}\mathbf{y}^H|\mathbf{S}, g_i, h_i\right] &= E\left[abP_1\mathbf{S}\mathbf{H}\mathbf{H}^H\mathbf{S}^H + \mathbf{n}\mathbf{n}^H\right]. \end{aligned} \tag{24}$$

Since $m = n = R$, we have

$$E\left[\mathbf{H}\mathbf{H}^H|g_i, h_i\right] = \mathrm{diag}\left(\, \mathbf{\beta}_1 \;\; \mathbf{\beta}_2 \;\; \cdots \;\; \mathbf{\beta}_i \,\right). \tag{25}$$

In the formula, $\beta_i = \mathrm{diag}\left(|g_{1i}h_i|^2|g_{2i}h_i|^2 \ldots |g_{Ri}h_i|^2\right)$, $i = 1, 2, \ldots, R$.

$E[\mathbf{H}\mathbf{H}^H|g_i, h_i] = \mathbf{K}$ is set, and formula (23) and formula (25) are substituted into formula (24), and the covariance matrix of the received signal is expressed as follows:

$$E\left[\mathbf{y}\mathbf{y}^{\mathrm{H}}|\mathbf{S}, g_i, h_i\right] = \rho\mathbf{S}\mathbf{K}\mathbf{S}^H + \xi\mathbf{I}_T = \Gamma_y. \tag{26}$$

In the formula, $\rho = abP_1$ and it satisfies $\mathbf{S}\mathbf{S}^{\mathrm{H}} = t\mathbf{I}$.

Finally, the conditional probability density function under the partially coherent network can be obtained, which is expressed as follows:

$$P(\mathbf{y}|\mathbf{S}, g_i, h_i) = \frac{1}{\pi\left|\Gamma_y\right|}\exp\left[-\left(\mathbf{y}^H\Gamma_y^{-1}\mathbf{y}\right)\right]. \tag{27}$$

At the receiving end, the maximum likelihood is used for decoding, and the decoding decision information of the partially coherent distributed space-time code is obtained.

$$\widehat{\mathbf{S}} = \arg\max P(\mathbf{y}|\mathbf{S}, g_i, h_i). \tag{28}$$

According to the matrix inversion lemma, if the matrices $\mathbf{A} \in \mathbb{C}^{N\times N}, \mathbf{C} \in \mathbb{C}^{N\times N}$ are non-singular matrices, and the matrices are $\mathbf{B} \in \mathbb{C}^{N\times N}, \mathbf{D} \in \mathbb{C}^{N\times N}$, then the matrix $\mathbf{A} + \mathbf{BCD}$ has the inverse matrix $(\mathbf{A} + \mathbf{BCD})^{-1} = \mathbf{A}^{-1} - \mathbf{A}^{-1}\mathbf{B}(\mathbf{D}\mathbf{A}^{-1}\mathbf{B} + \mathbf{C}^{-1})^{-1}\mathbf{D}\mathbf{A}^{-1}$, and the equivalent formula $|\mathbf{I} + \mathbf{AB}| = |\mathbf{I} + \mathbf{BA}|$. We get

$$\Gamma_y^{-1} = \xi^{-1}\left(\mathbf{I} - \mathbf{S}\left(\rho^{-1}\xi\mathbf{I} - \mathbf{K}\right)^{-1}\mathbf{K}\mathbf{S}^{\mathbf{H}}\right). \tag{29}$$

Formula (28) simplifies to

$$\widehat{\mathbf{S}} = \arg\max\left(\mathbf{y}^H\mathbf{S}\left(\rho^{-1}\xi\mathbf{I} - \mathbf{K}\right)^{-1}\mathbf{K}\mathbf{S}^H\mathbf{y}\right). \tag{30}$$

Now, the simulation and comparison of the bit error rate performance of the partially coherent distributed space-time code under the multi-hop multi-relay cooperative communication system are carried out. The channel fading coefficient and noise are both independent and identically distributed complex Gaussian random variables with mean 0 and variance 1.

We assume that the unitary matrix selects 4 sets of different parameter matrices, which are, respectively, $v = [5555]$, $v = [1357]$, $v = [1111315]$, and $v = [551113]$. The simulation results are shown in Figure 6. It can be seen from the figure that under the same system model and the same L, the performance obtained by the selection of the unitary matrix parameters will also be different, and the selection of the parameter matrix has a greater impact on the system performance. To optimize the system performance, it is necessary to select an appropriate parameter matrix according to the actual situation during encoding.

The bit error rate performance of the proposed three-hop multi-relay distributed space-time code and the two-hop multi-relay system is simulated and compared. In the simulation, L16, the parameter matrix used is v551113. Comparison of bit error rate performance under multi-hop multi-relay and two-hop relay networks is shown in Figure 7, and the simulation results are shown in Figure 8. The simulation results show that the bit error rate of the two-hop communication system model is slightly better than that of the three-hop model under the condition of a low signal-to-noise ratio. However, the three-hop communication model is better than the two-hop under a high signal-to-noise ratio. When the bit error rate is 10–5, the difference between the two is about 3 dB.

We assume that the wireless communication system model is shown in Figure 9, which is a multisource two-hop distributed space-time code system with a total of $M + N + 1$ nodes. Among them, M source nodes are denoted as $S_i, i = 1, 2, \ldots, m, N$ relay nodes are denoted as $R_j, j = 1, 2, \ldots, n$ respectively, and a destination node is denoted as D. There is no direct link between source node S and destination node D. The channel coefficient from source node S_i to relay node R_j is denoted as f_{ij}, and the channel coefficient from relay

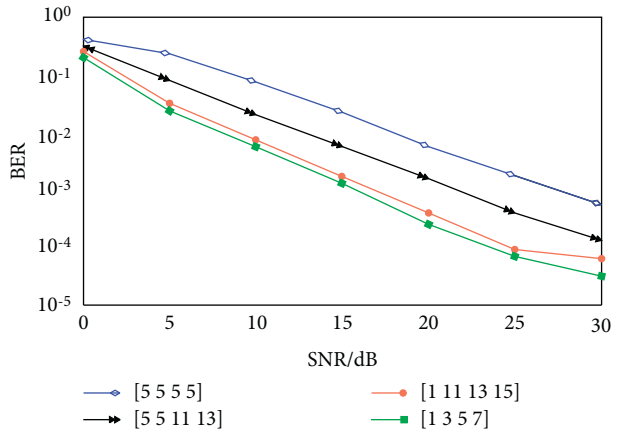

Figure 6: In the multi-hop multi-relay network, $L = 16$, the performance comparison under different parameter matrices.

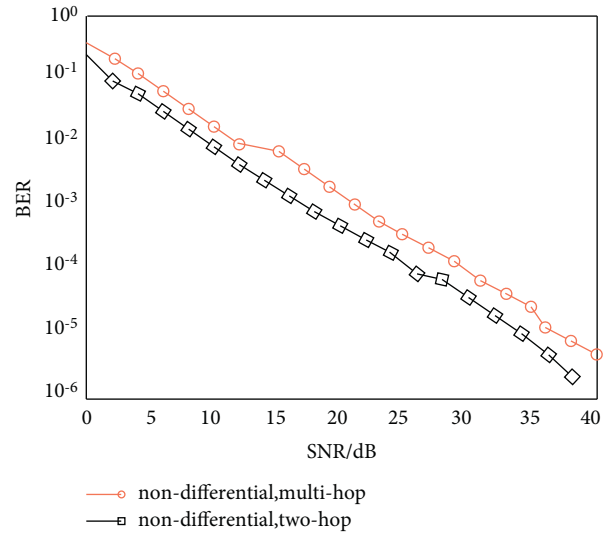

Figure 7: Comparison of bit error rate performance under multi-hop multi-relay and two-hop relay networks.

node R_j to destination node D is denoted as h_{jD}. We assume that the channel is a flat Rayleigh channel, all nodes are half-duplex, and they are synchronized at the symbol level, the channel coefficients f_{ij} and h_{jD} are independent of each other, and they obey a complex Gaussian distribution with mean 0 and variance 1.

The structure of the designed $2m \times m$ western space-time constellation diagram based on trigonometric functions is expressed as follows:

$$\mathbf{S}_l = \begin{bmatrix} \mathbf{S}_m \\ \mathbf{C}_m \end{bmatrix} = \begin{bmatrix} \sin\left(\frac{\pi l}{L}\right) \cdot \mathbf{I}_m \\ \cos\left(\frac{\pi l}{L}\right) \cdot \mathbf{I}_m \end{bmatrix}. \tag{31}$$

In the formula, $l = 0, 1, \ldots, L-1$, $\mathbf{S}_l$ represents the $l+1$th constellation matrix in the constellation diagram. Both $\mathbf{S}_m = \sin(\pi l/L) \cdot \mathbf{I}_m$ and $\mathbf{C}_m = \cos(\pi l/L) \cdot \mathbf{I}_m$ are diagonal matrices of $m \times m$, and the diagonal elements are $\sin(\pi l/L)$ and $\cos(\pi l/L)$, respectively.

The matrix in formula (31) satisfies the following formula:

$$\mathbf{S}_l{}^H \mathbf{S}_l = \mathbf{S}_m{}^2 + \mathbf{C}_m{}^2 = \sin^2\left(\frac{\pi l}{L}\right) \cdot \mathbf{I}_m{}^2 + \cos^2\left(\frac{\pi l}{L}\right) \cdot \mathbf{I}_m{}^2 = \mathbf{I}_m. \tag{32}$$

Therefore, the matrix is a west space-time matrix based on trigonometric functions.

In the relay phase, the signal received at the jth relay node R_j is as follows:

$$\begin{aligned} \mathbf{y}_{Rj} &= \mathbf{s}_1 f_{1j} + \mathbf{n}_{1j} + \mathbf{s}_2 f_{2j} + \mathbf{n}_{2j} + \cdots + \mathbf{s}_i f_{ij} + \mathbf{n}_{ij} \\ &= \mathbf{S} \cdot \begin{bmatrix} f_{1j} & f_{2j} & \cdots & f_{ij} \end{bmatrix}^{\mathrm{T}} + \mathbf{n}_j, i = 1, 2, \ldots, m, j = 1, 2, \ldots, n. \end{aligned} \tag{33}$$

In the formula, $\mathbf{S} = \begin{bmatrix} \mathbf{s}_1 & \mathbf{s}_2 & \cdots & \mathbf{s}_i \end{bmatrix}$ represents the signal code word matrix sent by the source node, and $\mathbf{s}_i$ is the column vector, which represents the element to be sent by each antenna of the source node.

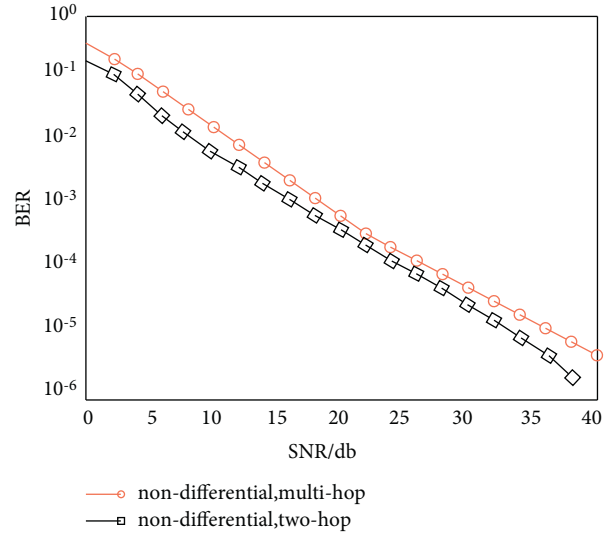

Figure 8: Performance simulation comparison of differential and non-differential coding under multi-hop and multi-relay.

The relay node firstly performs maximum-likelihood decoding on the received signal $\mathbf{y}_{R_j}$ and decodes to obtain the signal $\mathbf{S}'_{lj}$. If the decoding is correct, the decoded information is re-encoded to obtain a new code word matrix $\widetilde{\mathbf{S}}'_{lj}$ and then forwarded. If the decoding is wrong, it will not be forwarded.

No matter what kind of relay processing method is used, the signal processed by the relay node is uniformly expressed as follows:

$$\mathbf{Y} = \begin{bmatrix} \mathbf{A}_{m \times n} & \mathbf{B}_{m \times n} \end{bmatrix}^T. \tag{34}$$

The system block diagram of the destination receiver firstly combines the signal code words sent by the relay node using the maximum ratio combining method and then performs west space-time demodulation, and finally, it inversely maps the corresponding bit sequence. The signal

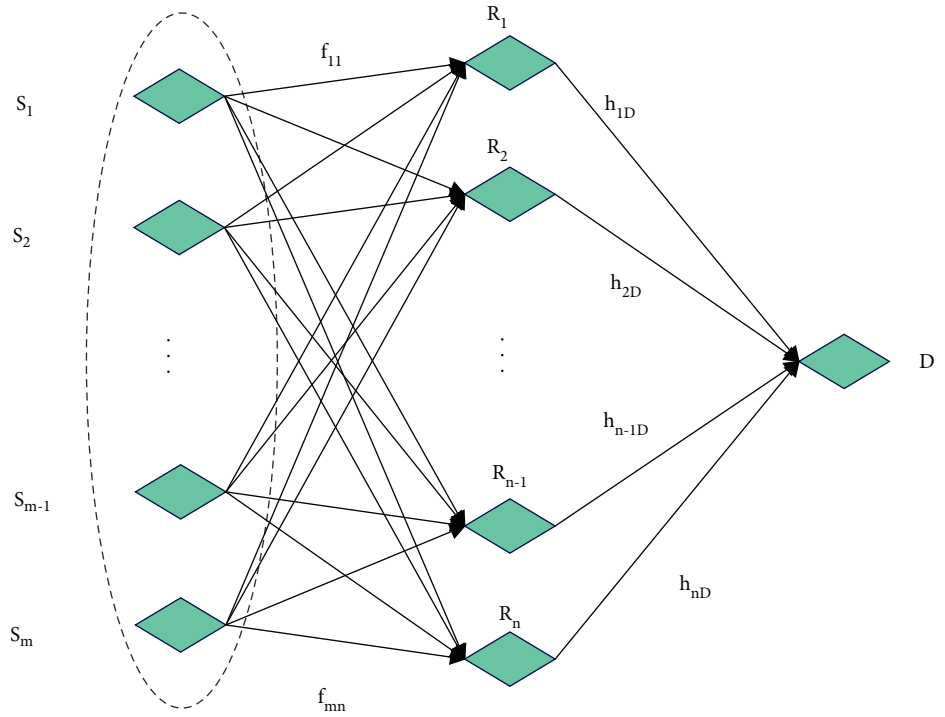

Figure 9: Multisource two-hop distributed space-time code system model.

information received by the receiver under the two cooperation modes will be different, which are as follows:

(1) In AF cooperation mode, the signal received by the destination receiver is as follows:

$$\mathbf{y}_D = \sum_{j=1}^{n} h_{jD}\mathbf{y}'_{R_j} + \mathbf{w}_D. \tag{35}$$

In the formula, $\mathbf{w}_D$ is the additive white Gaussian noise at the destination receiver.

(2) In DF cooperation mode, the signal received by the receiver is as follows:

$$\mathbf{y}_D = \sum_{j=1}^{n} h_{jD}\widetilde{\mathbf{S}}'_{lj} + \mathbf{w}_D. \tag{36}$$

In the formula, $\mathbf{w}_D$ is the additive white Gaussian noise at the destination receiving end.

When the transmitted signal is S, the conditional probability density of the received signal is shown in formula (39). Therefore, when the channel fading factor is unknown, the destination node adopts the maximum-likelihood decoding:

$$\widehat{\mathbf{S}} = \arg\max p(\mathbf{Y}|\mathbf{S}) = \arg\max \frac{\exp\left(-tr\left\{\mathbf{\Lambda}^{-1}\mathbf{Y}\mathbf{Y}^H\right\}\right)}{\pi|\mathbf{\Lambda}|}. \tag{37}$$

In the formula, $p(\mathbf{Y}|\mathbf{S})$ is the conditional probability that the receiving matrix is Y when the transmitting signal is $\mathbf{S}$. tr represents the trace of the matrix, $\Lambda = \mathbf{I}_T + \mathbf{S}\mathbf{S}^H$.

Formula (37) describes the maximum-likelihood decoding algorithm for western space-time modulation. Because of the special structure of the constellation diagram proposed in this study, its ML demodulation algorithm can be simplified.

We assume that the transmitted signal matrix is $\mathbf{S}_l$, $\mathbf{Y}$ is the corresponding receiving matrix, and formula (37) can be simplified to obtain the decision signal of the WST modulation:

$$\widehat{\mathbf{S}}_{ML} = \text{argmax}_{\mathbf{S}_l \in (\mathbf{s}_0,\ldots,\mathbf{s}_{l-1})} tr\left\{\mathbf{Y}^H\mathbf{S}_l{\mathbf{S}_l}^H\mathbf{Y}\right\}. \tag{38}$$

To facilitate the calculation, at the destination node, the receiving matrix Y is written as follows:

$$\mathbf{Y} = \left[\begin{array}{cc}\mathbf{\Phi}_s & \mathbf{\Phi}_c\end{array}\right]^T. \tag{39}$$

In the formula, Φ_s and Φ_c are both $m \times 1$ matrices, because there is only one antenna in the design of the receiving node in the system model. The maximum-likelihood demodulation algorithm can be obtained by substituting formula (31) and formula (39) into formula (38), and the derivation process is as follows:

$$\text{argmax}_{\mathbf{S}_l \in (\mathbf{s}_0,\ldots,\mathbf{s}_{L-1})} tr\left\{\mathbf{Y}^H\mathbf{S}_l{\mathbf{S}_l}^H\mathbf{Y}\right\} = \text{argmax}_{l\in[0,\ldots,L-1]} tr\left\{\left|\mathbf{\Phi}_s\right|\sin\left(\frac{\pi l}{L}\right) + \left|\mathbf{\Phi}_c\right|\cos\left(\frac{\pi l}{L}\right)\right\}^2. \tag{40}$$

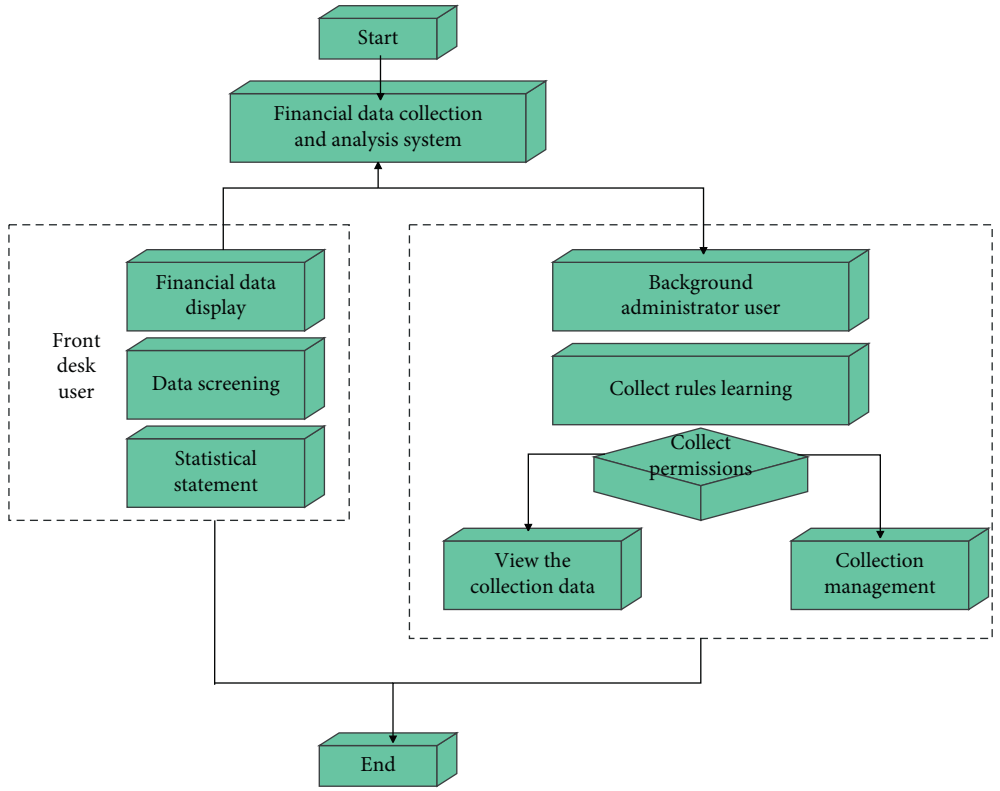

Figure 10: System business flow chart.

Therefore, the following formula (41) can obtain the $l \in [0, \ldots, L-1]$ search of the maximum value, as follows:

$$tr\left\{\left|\mathbf{\Phi}_s\right|\sin\left(\frac{\pi l}{L}\right)+\left|\mathbf{\Phi}_c\right|\cos\left(\frac{\pi l}{L}\right)\right\}^2. \tag{41}$$

According to the transformation relationship of trigonometric functions, there are as follows:

$$(A\ \sin\ \alpha + B\ \cos\ \alpha)^2 = \frac{A^2+B^2}{2}+\frac{B^2-A^2}{2}\cos\ 2\ \alpha + AB\ \sin\ 2\ \alpha. \tag{42}$$

Formula (41) can be written as follows:

$$\begin{aligned} &tr\left\{\left|\mathbf{\Phi}_s\right|\sin\left(\frac{\pi l}{L}\right)+\left|\mathbf{\Phi}_c\right|\cos\left(\frac{\pi l}{L}\right)\right\} \\ &= tr\left\{\frac{\left|\mathbf{\Phi}_s\right|^2+\left|\mathbf{\Phi}_c\right|^2}{2}+\frac{\left|\mathbf{\Phi}_s\right|^2-\left|\mathbf{\Phi}_c\right|^2}{2}\cos\left(\frac{2\pi l}{L}\right)+\mathrm{Re}\left(\mathbf{\Phi}_c\mathbf{\Phi}_s{}^{\mathrm{H}}\right)\sin\left(\frac{2\pi l}{L}\right)\right\}. \end{aligned} \tag{43}$$

After further simplification, formula (38) can be expressed as follows:

$$\begin{aligned} \widehat{\mathbf{S}}_{ML} &= \mathrm{argmax}_{\mathbf{S}_\ell\in(\mathbf{s}_0,\ldots,\mathbf{s}_{L-1})} tr\left\{\mathbf{Y}^H\mathbf{S}_l\mathbf{S}_l{}^H\mathbf{Y}\right\} \\ &= \mathrm{argmax}_{l\in[0,\ldots,-1]}\left[a\ \cos\left(\frac{2\pi l}{L}\right)+b\ \sin\left(\frac{2\pi l}{L}\right)\right] \\ &= \mathrm{argmax}_{l\in[0,\ldots,L-1]}\left(\xi\ \cos\left(\frac{\varphi-2\pi l}{L}\right)\right). \end{aligned} \tag{44}$$

In the formula, $\xi = \sqrt{b^2+a^2}$, $\varphi = \arctan(b/a)$, $a = \sum_{i=0}^{m-1} |\Phi_{ci}|^2 - |\Phi_{si}|^2/2$, $b = \mathrm{Re}(\sum_{i=0}^{m-1}\Phi_{ci}\Phi_{si}{}^H)$, and Φ_{si} and Φ_{ci}, respectively, represent the ith row element in the receiving matrix, where $i = 1, 2, \ldots, m$. Therefore, formula (44) can be understood as finding $l \in [0, \ldots, L-1]$ to make the following function achieve the maximum value:

$$f(l) = \xi\ \cos\left(\frac{\varphi-2\pi l}{L}\right). \tag{45}$$

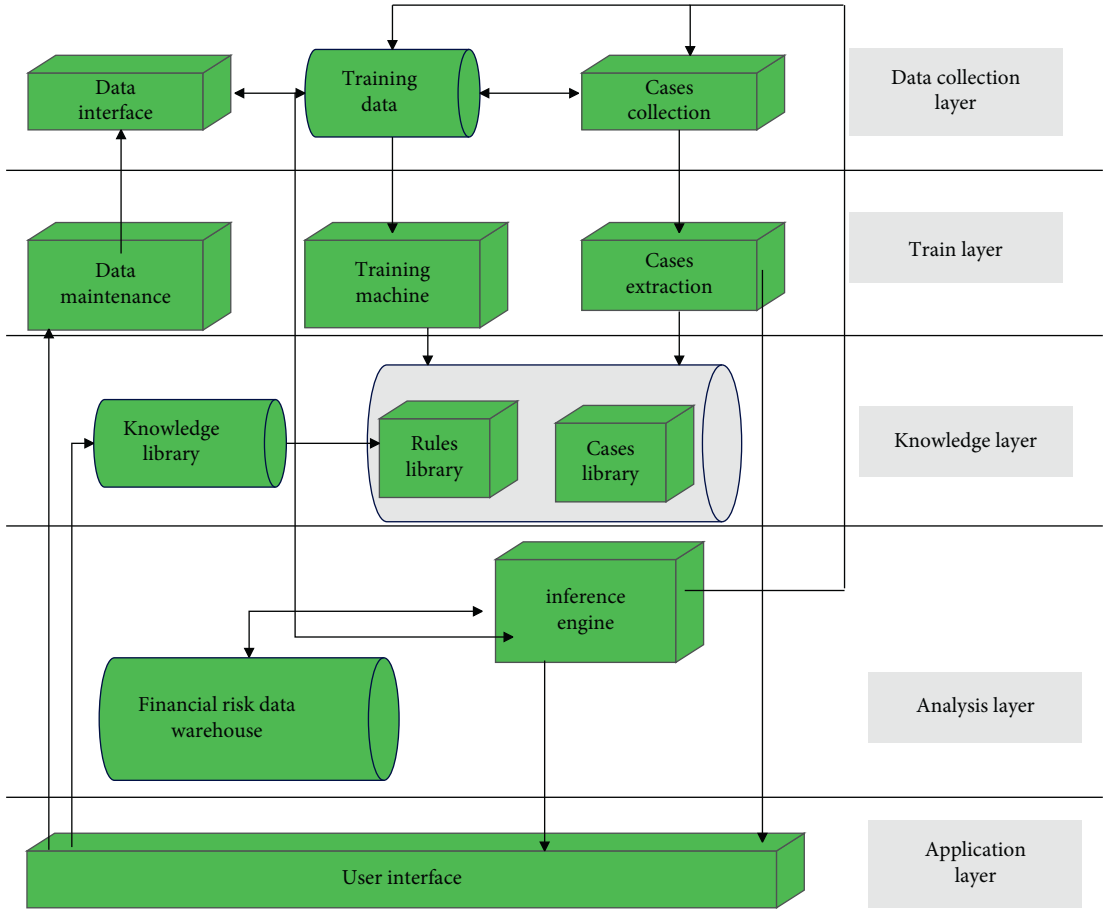

Figure 11: Overall system model.

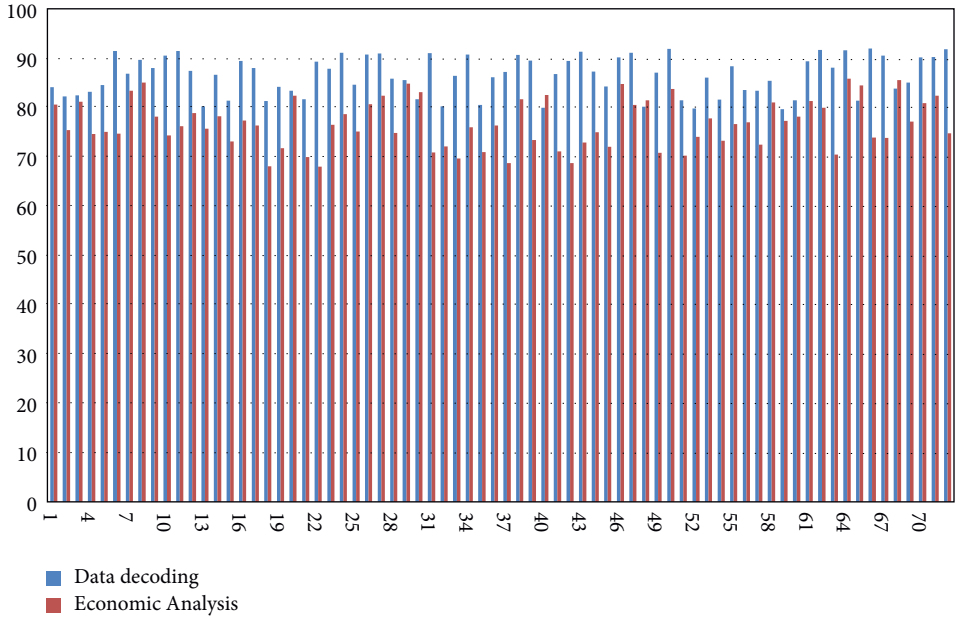

Figure 12: Experimental verification of regional financial and economic data processing system based on distributed decoding technology.

Observing formula (45), it can be seen that to make the function $f(l)$ achieve the maximum value, only $\cos(\varphi - 2\pi l/L) = 1$; that is, $l = \varphi L/2\pi$. Therefore, the decoding algorithm only needs to know the value of l to determine the signal to be sent.

4. Regional Financial Economic Data Processing Based on Distributed Decoding Technology

The whole mining query system is composed of two parts, the client module and the server module, and adopts the typical B/S mode. The system administrator directly logs in to the background of the financial data mining system through the URL address for data mining management. Moreover, ordinary users in the foreground view the mined data through the data display page. The business flow chart of the system is shown in Figure 10.

Financial data analysis includes two levels of individual analysis and regional analysis. Among them, the individual analysis obtains the potential financial risk factors for a single financial institution by analyzing the operational data and external environment of the individual financial institution. Regional analysis analyzes the operation data and external environment of all financial institutions in a certain region and combines the results of individual analysis to obtain regional financial risk assessment in a certain region. This study focuses on individual risk analysis and introduces external environmental data of financial institutions into individual risk analysis. The overall model design of the system is shown in Figure 11.

The model proposed in this study uses the distributed decoding technique described above for data processing. Through the simulation test of MATLAB, the financial data processing and economic analysis effect of the system in this study are verified, and the results shown in Figure 12 are obtained.

It can be seen from the experimental analysis that the regional financial and economic data processing system based on distributed decoding technology proposed in this study can play an important role in the analysis of financial and economic data.

5. Conclusion

Due to the specific economic meaning contained in the data itself in financial data, a single data-based clustering method can effectively classify the data, thereby effectively assisting domain experts to observe and analyze the initial data. However, due to the large scale of financial data, the results of clustered parallel coordinates are still messy and difficult to distinguish, which brings great challenges to further identifying the characteristics and trends of each classification. This study combines distributed decoding technology to construct a regional financial data processing system to improve the effect of regional financial data processing. The experimental analysis shows that the regional financial and economic data processing system based on distributed decoding technology proposed in this study can play an important role in the analysis of financial and economic data.

Data Availability

The labeled dataset used to support the findings of this study is available from the author upon request.

Conflicts of Interest

The author declares no conflicts of interest.

Acknowledgments

This study was sponsored by the Yellow River Conservancy Technical Institute.

References

[1] T. Abou-Chadi and T. Kurer, "Economic risk within the household and voting for the radical right," *World Politics*, vol. 73, no. 3, pp. 482–511, 2021.

[2] T. R. Chowdhury, S. Chakrabarty, M. Rakib, S. Saltmarsh, and K. A. Davis, "Socio-economic risk factors for early childhood underweight in Bangladesh," *Globalization and Health*, vol. 14, no. 1, pp. 54–12, 2018.

[3] E. Asare, A. K. Hoshide, F. A. Drummond, G. K. Criner, and X. Chen, "Economic risk of bee pollination in Maine wild blueberry, Vaccinium angustifolium," *Journal of Economic Entomology*, vol. 110, no. 5, pp. 1980–1992, 2017.

[4] F. Rodriguez, T. Toulkeridis, W. Sandoval, O. Padilla, and F. Mato, "Economic risk assessment of Cotopaxi volcano, Ecuador, in case of a future lahar emplacement," *Natural Hazards*, vol. 85, no. 1, pp. 605–618, 2017.

[5] B. J. Galli and G. Battiloro, "Economic decision-making and the impact of risk management: how they relate to each other," *International Journal of Service Science, Management, Engineering, and Technology*, vol. 10, no. 3, pp. 1–13, 2019.

[6] J. Belás, L. Smrcka, B. Gavurova, and J. Dvorsky, "The impact of social and economic factors in the credit risk management of SME," *Technological and Economic Development of Economy*, vol. 24, no. 3, pp. 1215–1230, 2018.

[7] S. Chakrabarti, M. T. Khan, A. Kishore, D. Roy, and S. P. Scott, "Risk of acute respiratory infection from crop burning in India: estimating disease burden and economic welfare from satellite and national health survey data for 250 000 persons," *International Journal of Epidemiology*, vol. 48, no. 4, pp. 1113–1124, 2019.

[8] K. Peng, M. Tian, M. Andersen et al., "Incidence, risk factors and economic burden of fall-related injuries in older Chinese people: a systematic review," *Injury Prevention : Journal of the International Society for Child and Adolescent Injury Prevention*, vol. 25, no. 1, pp. 4–12, 2019.

[9] J. E. Laine, V. T. Baltar, S. Stringhini et al., "Reducing socioeconomic inequalities in all-cause mortality: a counterfactual mediation approach," *International Journal of Epidemiology*, vol. 49, no. 2, pp. 497–510, 2020.

[10] C. O'Connell, M. Motallebi, D. L. Osmond, and D. L. Hoag, "Trading on risk: the moral logics and economic reasoning of North Carolina farmers in water quality trading markets," *Economic Anthropology*, vol. 4, no. 2, pp. 225–238, 2017.

[11] J. Odehnal and J. Neubauer, "Economic, security, and political determinants of military spending in NATO countries," *Defence and Peace Economics*, vol. 31, no. 5, pp. 517–531, 2020.
[12] K. Broekhuizen, D. Simmons, R. Devlieger et al., "Cost-effectiveness of healthy eating and/or physical activity promotion in pregnant women at increased risk of gestational diabetes mellitus: economic evaluation alongside the DALI study, a European multicenter randomized controlled trial," *International Journal of Behavioral Nutrition and Physical Activity*, vol. 15, no. 1, pp. 23–12, 2018.
[13] N. R. Mosteanu, "The influence of financial markets on countries' economic life," *Economics World*, vol. 5, no. 3, pp. 268–280, 2017.
[14] A. Qiu, M. Shen, C. Buss et al., "Effects of antenatal maternal depressive symptoms and socio-economic status on neonatal brain development are modulated by genetic risk," *Cerebral Cortex*, vol. 27, no. 5, pp. 3080–3092, 2017.
[15] T. Haer, W. W. Botzen, J. Zavala-Hidalgo, C. Cusell, and P. J. Ward, "Economic evaluation of climate risk adaptation strategies: cost-benefit analysis of flood protection in Tabasco, Mexico," *Atmósfera*, vol. 30, no. 2, pp. 101–120, 2017.
[16] P. Pan, D. Chao, and Q. Yu, "Economic policy uncertainty, bank risk-taking and firm investment," *Journal of Finance and Economics*, vol. 46, no. 02, pp. 67–81, 2020.
[17] J. B. Carr, C. V. Hawkins, and D. E. Westberg, "An exploration of collaboration risk in joint ventures: perceptions of risk by local economic development officials," *Economic Development Quarterly*, vol. 31, no. 3, pp. 210–227, 2017.
[18] S. S. Mirza and T. Ahsan, "Corporates' strategic responses to economic policy uncertainty in China," *Business Strategy and the Environment*, vol. 29, no. 2, pp. 375–389, 2020.
[19] T. D. van der Pol, E. C. van Ierland, and S. Gabbert, "Economic analysis of adaptive strategies for flood risk management under climate change," *Mitigation and Adaptation Strategies for Global Change*, vol. 22, no. 2, pp. 267–285, 2017.